ORIGINAL PAPER

Molecule design and screening of novel unsymmetrical zinc phthalocyanine sensitizers for dye-sensitized solar cells

Hongji Cui · Ruimin Ma · Ping Guo · Qinghua Zeng · Guoqun Liu · Xianxi Zhang

Abstract The molecular orbital and optical properties of the dyes PCH001 and TT1 reported previously were studied using the density functional theory (DFT) and time-dependent density functional theory (TDDFT) calculations. The results show that the electronic spectra simulated for PCH001 and TT1 in ethanol were in good agreement with the experimental data. The molecular orbital spatial orientation was used to interpret the discrepancy of the photovoltaic performances of the PCH001 and TT1 sensitized solar cells. The conjugation between the carboxyl group and the phthalocyanine ring in TT1 was found to be better than that through the C-C single bond in PCH001, which may contribute to TT1's improved performance. Four new unsymmetrical phthalocyanine molecules with the peripheral substituents as donors and anchoring groups as acceptors, namely CZ1, CZ2, *trans*- and *cis*-CZ3, were designed and compared to PCH001 and TT1. The new molecules CZ2 and *cis*-CZ3 were promising and may challenge the current record of PCH001 and TT1 in phthalocyanine-sensitized solar cells.

H. Cui · R. Ma · P. Guo · Q. Zeng · X. Zhang (✉)
School of Chemistry and Chemical Engineering,
Liaocheng University,
Liaocheng 252059, China
e-mail: zhangxianxi@lcu.edu.cn

Q. Zeng
School of Agriculture, Liaocheng University,
Liaocheng 252059, China

G. Liu (✉)
School of Materials and Chemical Engineering,
Zhongyuan University of Technology,
Zhongyuan Road 41#,
Zhengzhou 450007, China
e-mail: flyskyliugq@126.com

Introduction

Dye-sensitized solar cells (DSSCs) have attracted significant attention as a low-cost alternative to the conventional solid-state photovoltaic devices [1–9]. The most successful charge-transfer sensitizers employed in these cells are the polypyridylruthenium complexes, which yield solar-to-electric power conversion efficiencies of 10–11% under simulated sunlight. In spite of this, the main drawback of the ruthenium based sensitizers is the lack of absorption in the red region of the visible spectrum [10]. However, phthalocyanine (Pc) and metallophthalocyanine (MPc) exhibit very high extinction coefficients around 700 nm. The redox features also make them especially suitable for integration in light energy conversion systems. Additionally, by making use of infrared light, the solar heating of the buildings is reduced, thereby reducing the demand and power consumption of the air conditioning units [11–14]. Moreover, the structures of Pc and MPc can be easily modified without significantly changing their stability and processability. The photophysical and photochemical properties of these complexes can be altered by introducing different substituents into the peripheral positions of the macrocyclic ring, varying the central metal ions, alternating the axial ligands, or changing the symmetry of the macrocycle [15–19].

Zinc phthalocyanines have been tested as sensitizers for the wide band gap oxide semiconductors. A novel unsymmetrical zinc phthalocyanine PCH001 sensitizer contains three tert–butyl and two carboxylic acid groups acting as " push " and " pull " groups, respectively [8]. The function of these two carboxylic acid groups is to graft the

sensitizer onto the semiconductor surface and provide intimate electronic coupling between the excited state of the sensitizer and the conduction band of the semiconductor. The PCH001-sensitized solar cell yields a 75% maximum incident photon-to-current conversion efficiency (IPCE) with a 3.05% power conversion efficiency (η) under one-sun simulated solar irradiation when incorporated into a liquid electrolyte cell [8]. PCH003 has six butyloxy groups that act as electron donors [9], which further extends the 'push-pull' concept. The butyloxy groups also further enhance the solubility of phthalocyanine in the common organic solvents. Due to the poor electron injection rate of PCH003, the IPCE of 25% and the power conversion efficiency of 1.13% were observed under one-sun simulated solar irradiation by using a liquid electrolyte. Another unsymmetrical zinc phthalocyanine TT1 with three tert-butyl groups and a carboxyl group linked directly to the Pc ring was synthesized to further challenge the IPCE. This compound showed 80% IPCE at 690 nm and a record efficiency of 3.52% under one-sun [20].

In this paper, the PCH001 and TT1 sensitizers were investigated using the density functional theory (DFT) and time-dependent density functional theory (TDDFT) method. The tert–butyl groups on PCH001 and TT1 were replaced by the methyl groups to reduce the calculation load (See molecular structures in Fig. 1). The molecular orbital spatial orientations of PCH001 and TT1 are discussed to explain the discrepancy of the essential properties as sensitizers.

Four new molecular structures were also designed to find appropriate candidates for making improved solar cells.

CZ1 has three methoxyl groups attached to the Pc ring instead of three methyl groups to further enhance the donor and the solubility of PCH001. The methyl groups connected to the oxygen atoms may also be replaced by tert-butyl groups in an actual synthesis. Introducing three amino groups to the donor moiety of the Pc ring of PCH001 results in the structure of CZ2. CZ3 has the ethinyl group being introduced to the bridge of PCH001 to further extend the π-conjugation system (Fig. 1). *Trans*-CZ3 and *cis*-CZ3 are isomers owing to the unsaturated bond existed between the phthalocyanine ring and the substituent. Through comparing these new molecules to those two dyes with known solar cell efficiencies, it is possible to identify candidate complexes that may be used for developing more efficient DSSCs.

Theory and methods

The ground state geometries of PCH001, TT1, CZ1, CZ2 and CZ3 were optimized at B3LYP level with LANL2DZ basis set using Gaussian 03 program [21]. The optical properties were examined using time-dependent density functional theory (TDDFT) method. For analyzing the energy matching between the sensitizers and the TiO_2 semiconductor, the energy levels of the molecular orbital for PCH001, TT1, CZ1, CZ2 and CZ3 were also computed at the B3LYP/3–21G* level in water, which is the same environment in the reported calculations of TiO_2 cluster. The solvent effect was evaluated using the polarizable continuum model (PCM) [22].

Fig. 1 Molecular structures of PCH001, TT1, CZ1, CZ2 and CZ3

R= -C(CH$_3$)$_3$, (PCH001)
R= -OC(CH$_3$)$_3$, (CZ1)
R= -NH$_2$, (CZ2)

TT1

cis-CZ3

trans-CZ3
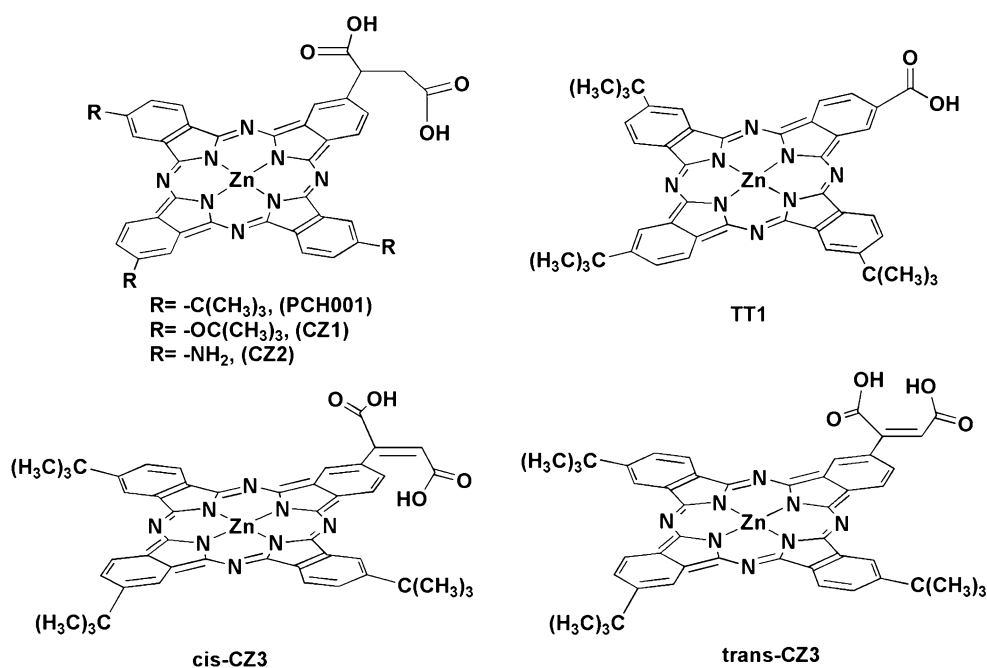
Results and discussion

The electronic structures of the ground state

DFT calculations with LANL2DZ basis set were employed to gain insight into the equilibrium geometries and the electronic structures for the frontier orbital of PCH001, TT1, CZ1, CZ2 and CZ3. No imaginary frequency is observed, indicating that the optimized geometries are in the global energy minima. The molecular orbital energy levels and the spatial orientations of the orbital for these complexes were shown in Figs. 2 and 3, respectively.

The peripheral substituents attached to the phthalocyanine ring of PCH001, CZ1 and CZ2 are different. These different substituents also vary the molecular orbital energy levels, the energy gaps between the highest occupied molecular orbital (HOMO) and the lowest unoccupied molecular orbital (LUMO), and the spatial orientation of the molecular orbital of these molecules.

As seen from Fig. 2, the molecular orbital energy levels rise along the variation of the peripheral substituents from the methyl group to the methoxyl and the amino groups. The HOMO of PCH001, CZ1 and CZ2 are essentially isolated from the HOMO-1, which lie at 1.49, 1.02 and 0.86 eV below the HOMO. However, the LUMO of these molecules are not energetically isolated, with the LUMO+ 1 only less than 0.1 eV above the LUMO. The HOMO energy level of CZ1 is located at −5.02 eV, which is about 0.15 eV above that of PCH001. The HOMO energy level of CZ2 is located at −4.72 eV, which is about 0.45 eV above that of PCH001. The LUMO of CZ1 and CZ2 are also higher than that of PCH001. This indicates that the energy difference between the LUMO of CZ1 and CZ2 and the conduction band of the semiconductor is larger than that of PCH001, which may thus provide better electron injection performance than PCH001.

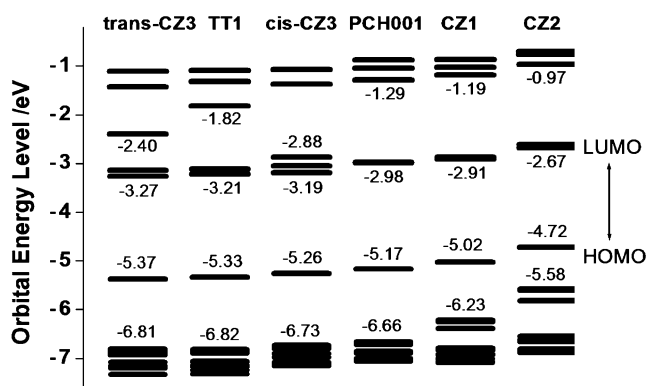In comparison with these three dyes, CZ1 and CZ2 show the narrower HOMO-LUMO gap than that of PCH001,

which is a benefit for absorbing the longer-wavelength light. Thus more photons can be absorbed at the same time, which may contribute to obtaining higher short circuit current density *Jsc* and overall power conversion efficiency η. It is also indicated from Fig. 2 that the redox potential of the dye was quite sensitive to the substitution of the functional group, which agrees with the result in the experiment [23].

As shown in Fig. 3, the HOMO of PCH001 is delocalized over the entire molecule. The LUMO of PCH001 is a π* orbital delocalized across the phthalocyanine ring and moved to the carboxyl group. The LUMO+ 3 is a π* orbital that is mainly localized over the phthalocyanine ring and further moved to the carboxyl group. This indicates that the photoexcited electrons transfer from the phthalocyanine skeleton to the carboxyl group, which is a benefit to the injection of the photoexcited electrons to the conduction band of the semiconductor. Similar distribution were also observed for the new molecules CZ1 and CZ2, indicating that these molecules may also provide efficient electron injection into the conduction band of the semiconductor.

Moreover, the peripheral substituent also plays an important role in the solubility and reduced aggregation of zinc phthalocyanine complexes used in the dye sensitized solar cells [10, 24]. This functionality may also be employed in the new molecules.

Besides the peripheral substituents, the anchoring groups also influence the properties of the sensitizers. The dyes bind strongly to the TiO₂ surface to ensure an efficient electron injection into the TiO₂ conduction band through an anchoring group, which are typically the carboxylate or the phosphonate groups. The link between the phthalocyanine and the anchoring group changes the energy level and the spatial orientation of the molecular orbital, which further influences the efficiency of the charge-separated state.

The conjugated chain instead of the saturated chain between the phthalocyanine ring and the anchoring group for CZ3 declines the orbital energy level with respect to that of PCH001. The HOMO energy levels of *trans*-CZ3 and *cis*-CZ3 are located at −5.37 and −5.24 eV, respectively, which are 0.2 and 0.09 eV below the HOMO energy level of PCH001. Moreover, the energy levels from HOMO to HOMO-4 for trans-CZ3 are slightly lower than those of cis-CZ3. The isomer effect for *trans*-CZ3 and *cis*-CZ3 does not lead to significant changes in the occupied orbital energy levels as shown in Fig. 2.

The LUMO and LUMO+ 1 orbital for PCH001, which are almost degenerate, are located at −2.98 eV. The five lowest unoccupied molecular orbitals of *trans*-CZ3 and *cis*-CZ3 isomers were isolated orbitals. The energy levels of these five unoccupied orbitals are lower than those of PCH001, but similar to those of TT1 owing to the enhanced
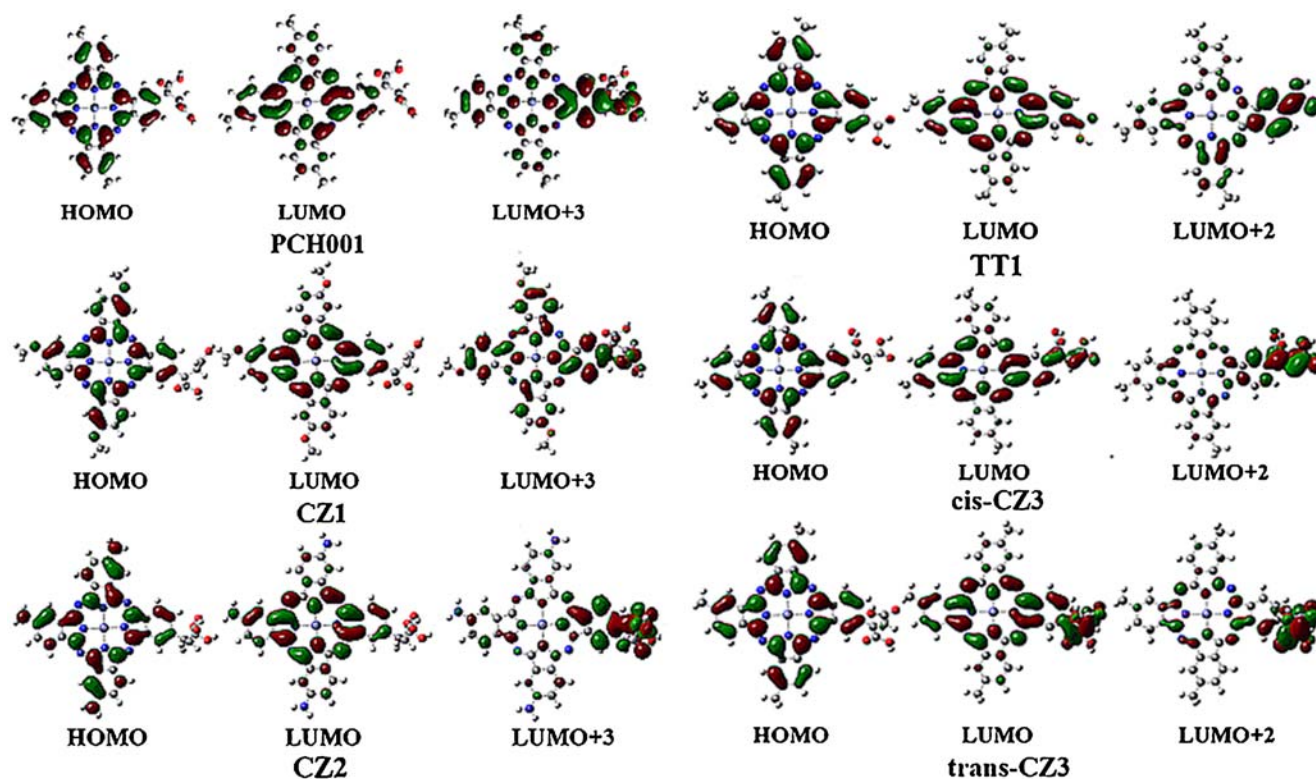

Fig. 2 Schematic representation of MO energy levels of PCH001, TT1, CZ1, CZ2 and CZ3

Fig. 3 Molecular orbital spatial orientation of PCH001, TT1, CZ1, CZ2 and CZ3

delocalization of π electrons caused by the unsaturated bond. In particular, the energy level of LUMO+ 2 is about 1.59 eV for *trans*-CZ3 and 1.11 eV for *cis*-CZ3 below that of PCH001. The anchoring group as acceptor moiety mainly regulates the unoccupied molecular orbital energy level, which further affects the injection efficiency of the photoexcited electrons to the conduction band of the semiconductor in the anode.

The carboxyl group contributes a lot to the LUMO of TT1, while not so much to the LUMO of PCH001 as shown in Fig. 3. This may be the reason that the performance of TT1 is better than PCH001 since most of the photoexcited electrons injected from the LUMO of the sensitizer into the conduction band of the semiconductor through the carboxyl group. Similar distributions were also observed for CZ3 as shown in Fig. 3, which indicates that CZ3 may also provide a good photoexcited electron transfer channel, and thus a good photon-to-current conversion efficiency.

Moreover, the HOMO-LUMO gaps of CZ3 are smaller than that of TT1, indicating that the light at longer-wavelengths may also be absorbed and contribute more to the short circuit current density *Jsc* and thus improve the photon-to-current conversion efficiency η. CZ3 dyes are thus promising to challenge the current record of TT1.

In this section, the results of orbital spatial orientation provide a good explanation for the overall conversion efficiency (η) difference of PCH001 and TT1. The variation

of the attachment pattern of acceptor moieties may change the performance of zinc phthalocyanine-sensitized solar cell. The theoretical results also indicate that the properties of the substituent and the anchoring group are related to the HOMO of the donor and the LUMO of the acceptor. The donor moiety of the phthalocyanine skeleton and the acceptor moiety with the carboxylic acid group may be further designed in latter investigations. The donor-acceptor pairs will be constructed to be used for DSSC, which could provide real electronic and structural information about the interface between the dye molecule and the semiconductor.

Absorption spectra

The lowest 80 singlet -singlet excitations of these complexes were calculated with TD-DFT method in the solvent ethanol to gain further insight into the excited sates of the candidate dyes. The experimental and theoretical absorption spectra data of PCH001 and TT1 in the solvent ethanol were listed comparatively in Table 1. The lowest transitions are calculated to be 1.99 eV for PCH001 and 1.93 eV for TT1, which correspond to the charge–transfer excitations from the HOMO to the LUMO. The red–shift of the absorption maximum considered from the theory to the experiment may be related to the self-interaction error in TD-DFT arising through the electron transfer in the extended charge–transfer state [25].

Table 1 Selected lowest-excited energies (ΔE), absorption wavelengths, oscillator strengths (*f*), and domination excitation characters for low-lying singlet state of PCH001 and TT1 in ethanol

PCH001

state	main configuration	ΔE/eV and λ/nm	*f*	Excitation character	Exp
1	180[a] → 181[b] 62%	1.99 (622)	0.593	LLCT[c]	1.79[d]
2	180 → 182 62%	2.00 (620)	0.586	LLCT	
15	175 → 182 42%	3.46 (358)	0.155	LLCT	
	176 → 182 40%				
17	171 → 181 38%	3.56 (348)	0.949	LLCT	3.57[d]
	176 → 181 34%				
18	171 → 182 40%	3.56 (348)	0.955	LLCT	
	176 → 182 32%				
21	172 → 182 34%	3.63 (341)	0.149	LLCT	
	172 → 181 23%				
33	167 → 181 64%	4.24 (293)	0.195	LLCT	
49	172 → 183 28%	5.04 (246)	0.105	LLCT	
	180 → 192 27%				

TT1

state	main configuration	ΔE/eV and λ/nm	*f*	Excitation character	Exp
1	161[a] → 162[b] 62%	1.93(643)	0.631	LLCT	1.82[f]
2	161 → 163 63%	2.02(613)	0.562	LLCT	1.86[f]
9	158 → 162 57%	3.19(389)	0.193	LMCT[e]	
14	154 → 162 46%	3.45(360)	0.342	LLCT	
16	154 → 162 40%	3.49(355)	0.276	LLCT	3.54[f]
18	153 → 162 39%	3.56(349)	0.492	LLCT	
	157 → 162 36%				
19	154 → 163 52%	3.58(347)	0.460	LLCT	
20	156 → 163 34%	3.59(346)	0.156	LLCT	
23	152 → 162 31%	3.63(342)	0.174	LLCT	
24	153 → 163 39%	3.65(340)	0.146	LLCT	
27	152 → 162 41%	3.73(332)	0.186	LLCT	
	153 → 163 50%				
32	148 → 162 63%	4.19(296)	0.159	LLCT	
34	148 → 163 65%	4.29(289)	0.138	LLCT	

[a] HOMO; [b] LUMO; [c] LLCT: ligand to ligand charge transfer; [d] cited from literature [8]; [e] LMCT: ligand to metal charge transfer; [f] cited from literature [20]

The experimental spectrum of TT1 shows three main features, which are well reflected in the spectrum simulated. Those two almost equally intense bands are located at 1.82 and 1.86 eV, respectively. The intense peak at higher energy region is located at 3.54 eV. It is noticed that the agreement between theory and experiment is good both in terms of the band position and the relative intensity by comparing this experimental spectrum with those of PCH001 and TT1 calculated in the ethanol solution. This indicates that the B3LYP method with the basis set LANL2DZ provides an effective measure to predict the absorption spectra of the novel unsymmetrical zinc phthalocyanine complexes.

The most relevant transitions constituting each band for CZ1, CZ2 and CZ3 is discussed next, while the excitation energies with the relative oscillator strengths (*f*) are listed in Table 2 and shown in Fig. 4 in detail. The maximum absorption wavelength calculated for CZ2 and CZ3 red shift largely with respect to those of PCH001 and TT1. The bands found at 654 nm for *trans*-CZ3 and 667 nm for *cis*-CZ3 in the calculated spectrum are 34 nm and 45 nm red–shifted with respect to that of PCH001 at 622 nm. It is partly contributed from the narrower orbital energy gap on the excited state. The energy gaps between the HOMO and the LUMO are 2.11 eV for CZ1, 1.96 eV for CZ2, 2.09 eV for *trans*-CZ3 and *cis*-CZ3, while 2.11 eV, 2.19 eV for PCH001 and TT1, which are consistent with the variation trend of the absorption peaks. Longer wavelength light can then be absorbed and contribute to provide a larger short circuit current density *Jsc* and thus higher photon-to-current conversion efficiency η.

Results in the tables also show that the first transition state originates from the HOMO to the LUMO for all the complexes considered. The calculated transitions perform the π - π* features, as compared to the CT (charge transfer) excitation being related to the localized character of a π - π* excitation, which involves substantially overlapping orbitals [26]. The carboxyl group and the conjugated chain connected with the carboxyl group and the phthalocyanine ring in CZ3 significantly contribute to the unoccupied orbital, which plays an important role on the electron injection from the excited dye to the semiconductor. Therefore, these two isomers are possibly superior to the PCH001 and TT1 sensitizers.

The LUMO and LUMO+ 1 for PCH001 and CZ1 are degenerate orbitals as shown in Fig. 2. The relative intensities of absorption peaks for PCH001 and CZ1 shown in Fig. 4 are higher than those of the other unsymmetrical phthalocyanine complexes owing to the superposition effect. The LUMO and LUMO+ 1 are energetically isolated orbitals in the electron transition for TT1, CZ2 and CZ3. Therefore, the relevant transitions that originate from HOMO to LUMO or LUMO+ 1 occur as two isolated absorption peaks in the range of 600–700 nm. The isolated peaks at lower energy region were found at 643 and 613 nm for TT1. Similar behavior was found at 703 and 672 nm for CZ2, 667 and 617 nm for cis-CZ3, as well as 654 and

Table 2 Selected lowest-excited energies (ΔE), absorption wavelength, oscillator strengths (*f*), and domination excitation character for low-lying singlet state of CZ1, CZ2 and CZ3 in ethanol

	CZ1				CZ2		
state	main configuration	ΔE/eV And λ/nm	*f*	state	main configuration	ΔE/eV And λ/nm	*f*
1	192 [a] → 193 [b] 62%	1.93 (643)	0.588	1	180 [a] → 181[b] 62%	1.76 (703)	0.46
2	192 → 194 62%	1.96 (633)	0.626	2	180 → 182 62%	1.85 (672)	0.591
3	191 → 193 65%	2.81 (441)	0.059	3	179 → 181 63%	2.26 (549)	0.096
4	190 → 193 48%	2.83 (439)	0.014	4	178 → 181 60%	2.27 (546)	0.014
	190 → 194 43%	2.85(435)	0.05	7	177 → 181 66%	2.61(476)	0.314
5	191 → 194 43%			8	177 → 182 66%	2.65(467)	0.217
6	190 → 194 49%	2.91 (427)	0.005	16	176 → 182 55%	3.52 (352)	0.281
	190 → 193 46%			17	172 → 181 49%	3.56(349)	0.545
7	189 → 193 59%	3.03(410)	0.205	18	173 → 184 49%	3.62(343)	0.252
8	189 → 194 59%	3.04(408)	0.094	19	175 → 182 45%	3.63(341)	0.621
11	187 → 193 49%	3.31(375)	0.018	20	173 → 181 41%	3.65(340)	0.203
16	185 → 194 33%	3.56(348)	0.293	21	173 → 181 42%	3.65(339)	0.112
	184 → 193 32%			25	171 → 181 51%	3.73(332)	0.113
17	192 → 196 32%	3.58 (347)	0.662	36	167 → 181 58%	4.21(294)	0.268
18	192 → 196 50%	3.59 (345)	0.322	37	167 → 182 51%	4.24(293)	0.233
	cis -CZ3				*trans*-CZ3		
1	179[a] → 180[b] 63%	1.86(667)	0.496	1	179 [a] → 180[b] 63%	1.90 (654)	0.736
2	179 → 181 62%	2.01(617)	0.575	2	179 → 181 62%	2.02 (613)	0.56
3	179 → 182 65%	2.13(581)	0.167	3	179 → 182 68%	2.55 (485)	0.027
4	178 → 180 62%	3.01(412)	0.022	4	178 → 180 62%	2.96 (419)	0.022
5	178 → 181 54%	3.05(403)	0.021	5	177 → 180 43%	3.03 (409)	0.003
6	176 → 180 44%	3.12(397)	0.082	6	178 → 181 55%	3.06 (405)	0.018
7	175 → 180 39%	3.28(378)	0.155	7	176 → 180 50%	3.11 (399)	0.105
11	175 → 181 39%	3.38(367)	0.264	11	176 → 181 42%	3.25 (382)	0.163
14	172 → 180 33%	3.46(358)	0.237	16	175 → 181 34%	3.40 (365)	0.245
15	170 → 180 47%	3.48(356)	0.303	17	179 → 183 37%	3.48 (357)	0.526
20	170 → 180 32%	3.51(354)	0.209	18	171 → 181 50%	3.57 (347)	0.580

[a] HOMO; [b] LUMO
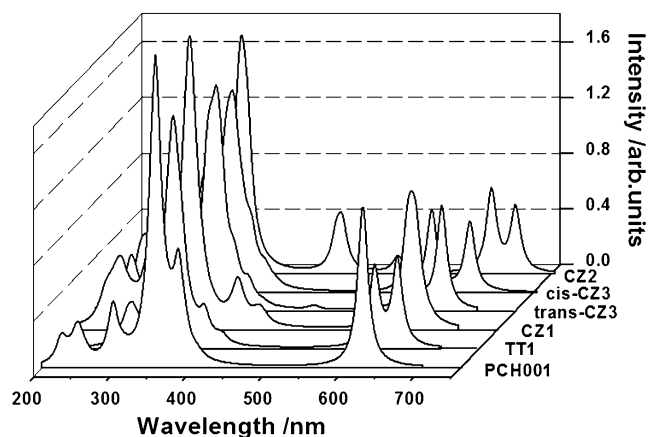
Fig. 4 Simulated spectra of PCH001, TT1, CZ1, CZ2 and CZ3
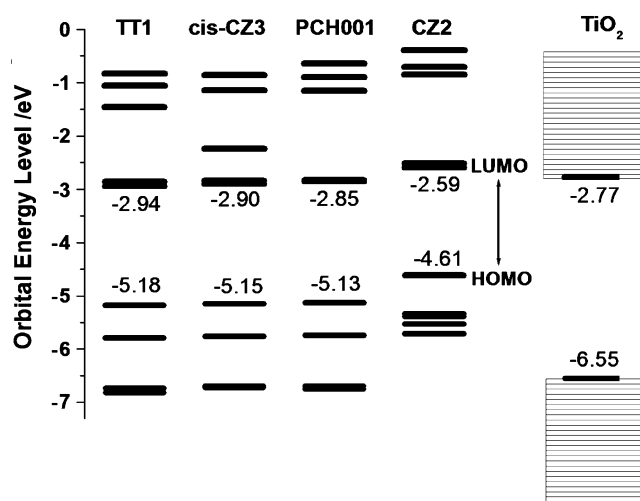
Fig. 5 Energy levels of PCH001, TT1, CZ1, CZ2 and CZ3 calculated at the B3LYP/3–21G* level in water and the results of a TiO₂ nanoparticle model

613 nm for *trans*-CZ3. A series of medium intensity peaks for CZ2 were also observed in the range of 450–550 nm. The novel CZ2 may provide better absorption across the whole spectral range, and thus provide better photon-to-current conversion performance.

Comparison of sensitizer and TiO$_2$ energy levels

The energy matching between the lowest unoccupied molecular orbital of the sensitizer and the band edge of the semiconductor TiO$_2$ is one of the key factors that influence the electron injection efficiency of DSSCs. The injection rate depends on the electronic properties of both the dye and the semiconductor. The distance between them as determined by the length of the molecular bridge also plays an important role [27]. The alignment of the energy levels for the unsymmetrical phthalocyanine complex with that of a TiO$_2$ nanoparticle model was analyzed to gain insight into the electronic factors. This TiO$_2$ nanoparticle model was made of a Ti$_{38}$O$_{76}$ cluster of nanometric dimensions exposing 101 anatase surfaces [28]. The HOMO and LUMO energies of the bare Ti$_{38}$O$_{76}$ cluster are calculated at −6.55 and −2.77 eV at the 3–21G* level in water, respectively. This results in a HOMO-LUMO gap of 3.78 eV [10, 28].

The absorption spectra of CZ2 and *cis*-CZ3 seem the best among the complexes designed. The energy matching between these sensitizers and the semiconductor were studied to further investigate the advantage of these two complexes as sensitizer with respect to PCH001 and TT1. The data for the sensitizers mentioned above were also obtained in the water solution at the B3LYP/3–21G* level for the sake of comparison. The molecular orbital energy levels are shown partly in Fig. 5. Only CZ2 has LUMO levels higher than that of the bare Ti$_{38}$O$_{76}$ cluster comparing the LUMO levels of PCH001, TT1 and candidate CZ2, *cis*-CZ3 with that of the cluster. Considering the systematic error of calculations between these two different types of complexes and cluster, more attention is paid on the trends rather than the absolute values. Since TT1 with the second lowest LUMO level among these complexes show very good photoexcited electron injection performance, the LUMO levels of the other complexes is still reasonable to be considered high enough to provide good electron injection performances.

The distances between those of the candidate sensitizers and that of the semiconductor cited above are approximately 0.18 eV, which is sufficient for the electron transfer [29]. CZ2 has a narrower HOMO-LUMO gap compared to that of PCH001, which has a known cell efficiency of 3.05%. This result suggests that CZ2 may be superior to the PCH001 sensitizer. The unsaturated bond introduced for *cis*-CZ3 reduces the distance between the LUMO or LUMO+ 2 and

the bare Ti$_{38}$O$_{76}$ cluster with respect to TT1. Moreover, the electron in LUMO+ 2 in the excited state for *cis*-CZ3 may effectively transfer to the semiconductor along the conjugative chain from the viewpoint of the molecular orbital spatial orientation. The CZ2 and *cis*-CZ3 complexes may be better sensitizers for developing efficient DSSCs.

Conclusions

The higher photovoltaic efficiency of TT1 with respect to that of PCH001 seems partly attributable to the good conjugation between the carboxyl group and the phthalocyanine ring, as judged by theoretical calculations presented here. The discrepancy of the IPCE for the dyes reported was also accurately reflected in the molecular orbital spatial orientation. Through the comparison between CZ1, CZ2 and PCH001 as well as CZ3 and TT1, it is shown that the electron injection efficiency of DSSC is correlated not only with the alignment of the three peripheral substituents, but also with the alignment of the unoccupied orbital as a final state of the electron transition. The new molecules CZ2 and *cis*-CZ3 are promising candidates and may challenge the current record of PCH001 and TT1 in the phthalocyanine-sensitized solar cells. Further experimental research to check the prediction of CZ2 or *cis*-CZ3 sensitized solar cells is in progress in our group.

References

1. Grätzel M (2001) Nature 414:338–344
2. Asbury JB, Ellingson RJ, Gosh HN et al (1999) J Phys Chem B 103:3110–3119
3. Heimer TA, Heilweil EJ, Bignozzi CA et al (2000) J Phys Chem A 104:4256–4262
4. Nazeeruddin MK (2004) Coord Chem Rev 248:1161–1164
5. Park NG, Kang MG, Kim KM et al (2004) Langmuir 20:4246–4253
6. Lee JJ, Coia GM, Lewis NS (2004) J Phys Chem B 108:5269–5281
7. Argazzi R, Larramona G, Contado C et al (2004) J Photochem Photobiol A 164:15–21
8. Reddy PY, Giribabu L, Lyness C et al (2007) Angew Chem Int Ed 46:373–376
9. Giribabu L, Vijaykumar C, Gopalreddy V et al (2007) Sol Energy Mater Sol Cells 91:1611–1617
10. Nazeeruddin MK, Angelis FD, Fantacci S et al (2005) J Am Chem Soc 127:16835–16847

11. Leznoff CC, Lever ABP (ed) (1993) Phthalocyanines: Properties and Application, VCH Publishers Inc 3:8
12. He JJ, Benko G, Korodi F et al (2002) J Am Chem Soc 124:4922–4932
13. He JJ, Hagfeldt A, Lindquist SE et al (2001) Langmuir 17:2743–2747
14. Escosura A, Martinez-DPaz MV, Torres T et al (2006) Chem Asian J 1:148–154
15. Li YJ, Pritchett TM, Huang JD et al (2008) J Phys Chem A 112:7200–7207
16. Micó XA, Vagin SI, Subramnian LR et al (2005) Eur J Org Chem 112:4328–4337
17. Chen Y, Hanack M, Araki Y et al (2005) Chem Soc Rev 34:517–529
18. Torre GDL, Vazquez P, Agullo-Lopez F et al (2004) Chem Rev 104:3723–3750
19. Nikolaitchik AV, Korth O, Rodgers MAJ (1999) J Phys Chem A 103:7587–7596
20. Cid JJ, Torres T, Yum JH et al (2007) Angew Chem Int Ed 46:8358–8362
21. Frisch MJ, Trucks GW, Schlegel HB et al (2003) Gaussian 03, Revision B.05. Gaussian Inc, Pittsburgh, PA
22. Miertus S, Tomasi J (1982) J Chem Phys 77:3654–3665
23. Kim D, Kang MS, Song K et al (2008) Tetrahedron 64:10417–10424
24. Rensmo H, Södergren S, Patthey L et al (1997) Chem Phys Lett 274:51–57
25. Xu W, Peng B, Chen J et al (2008) J Phys Chem C 112:874–880
26. Kim S, Lee JK, Kang SO et al (2006) J Am Chem Soc 128:16701–16707
27. Duncan WR, Stier WM, Prezhdo OV et al (2005) J Am Chem Soc 127:7941–7951
28. Fantacci S, Angelis FD, Sgamellotti N et al (2004) Chem Phys Lett 396:43–48
29. Tian HN, Yang XC, Chen RK et al (2008) J Phys Chem C 112:11023–11033